

AN ENTROPY SATISFYING FINITE VOLUME METHOD FOR THE FOKKER-PLANCK EQUATION OF FENE DUMBBELL MODEL

HAILIANG LIU AND HUI YU

ABSTRACT. In this paper, we propose a new entropy satisfying finite volume method to solve the Fokker-Planck equation of FENE dumbbell model for polymers, subject to homogeneous fluids. Both semi-discrete and fully discrete schemes satisfy all three desired properties: i) mass conservation, ii) positivity preserving, and iii) entropy satisfying. These ensure that the computed solution is a probability density, and converges to equilibrium as time evolves. Zero-flux at boundary is naturally incorporated, and boundary behavior is resolved sharply. Both one and two-dimensional numerical results are provided to demonstrate the good qualities of the scheme, as well as effects of some canonical homogeneous flows.

1. INTRODUCTION

Dumbbell models with finitely extensible nonlinear elastic (FENE) spring forces are now widely used in numerical flow calculations to capture nonlinear rheological phenomena, both in the classical approach via a closed constitutive equation, and in a modern approach in which the polymeric stress tensor is computed via Brownian dynamics (BD) simulations [5, 16]. For the dumbbell model the configuration probability density function (pdf) yields information on the probability of finding a dumbbell with a given configuration at a particular material point, hence solving the Fokker-Planck equation directly is desirable, as long as it is feasible [22].

The original empirical FENE spring potential

$$(1.1) \quad \Psi(m) = -\frac{Hb}{2} \log \left(1 - \frac{|m|^2}{b} \right),$$

was first proposed by Warner [24], where H is the spring constant, m is the d -dimensional connector vector of the beads with $m \in B := B(0, \sqrt{b})$, a ball in \mathbb{R}^d with radius \sqrt{b} denoting the maximum spring extension. It exhibits, for small extensions, the expected linear behavior and a finite length b in the limit of an infinite force.

This paper is concerned with the numerical solution of the Fokker-Planck equation of the FENE dumbbell model for the pdf $f = f(x, m, t)$,

$$(1.2) \quad \partial_t f + (v \cdot \nabla_x) f + \nabla_m \cdot (\nabla_x v m f) = \frac{2}{\zeta} \nabla_m \cdot (\nabla_m \Psi(m) f) + \frac{2k_B T}{\zeta} \Delta_m f,$$

where $x \in \mathbb{R}^d$ is the macroscopic Eulerian coordinate, and $v(x, t)$, the fluid velocity, is usually governed by the incompressible Navier-Stokes equation, ζ is the friction coefficient of the dumbbell beads, T is the absolute temperature, and k_B is the Boltzmann constant. We refer to Chaps 11 and 13 of [4] for a comprehensive survey of the physical background, and [8] for some augmented models with inertial forces.

Throughout this paper we consider only homogeneous flows. Therefore the velocity field of the fluid can be written as $v = \mathcal{K}x$, where $\mathcal{K} = \nabla v$ is independent of the position vector x in the fluid and has zero trace since we assume the fluid to be incompressible. Let the flow map be defined as

$$\partial_t X(y; t) = v(X(y; t), t), \quad X(y; 0) = y.$$

Date: March 25, 2011.

1991 Mathematics Subject Classification. 35K20, 65M08, 76A05, 82C31, 82D60.

Key words and phrases. Fokker Planck equations, FENE model, relative entropy, positivity preserving.

Along the flow map, with a suitable scaling, we arrive at the following equation for $f(m, t) := f(X(y; t), m, t)$ for each fixed y ,

$$(1.3a) \quad \partial_t f = \frac{1}{2} \nabla_m \cdot \left[\nabla_m f + \left(\frac{bm}{b - |m|^2} - 2\mathcal{K}m \right) f \right], \quad m \in B,$$

$$(1.3b) \quad f(m, 0) = f_0(m), \quad m \in B$$

$$(1.3c) \quad f = o(b - |m|^2), \quad \text{on } \partial B.$$

We remark that numerically one can also use operator splitting with respect to (m, t) , and (x, t) through solving another transport equation, $\partial_t f + \nabla \cdot (vf) = 0$. See [6, 7]. Boundary requirement (1.3c) is imposed to ensure the existence and uniqueness of the weak solution to (1.3) (see [18]).

The singularity of the Fokker-Planck equation near $|m| = \sqrt{b}$ makes the boundary issue rather subtle [17], and presents numerous challenges, both analytically and numerically. The regime of physical interest is $b > 2$, for which the boundary requirement (1.3c) was shown to be a sharp requirement for the solution to remain a probability density [18]. Moreover, this condition is equivalent to the zero flux boundary condition for $b > 2$ as shown in [18],

$$(1.4) \quad \left[\nabla_m f + \left(\frac{bm}{b - |m|^2} - 2\mathcal{K}m \right) f \right] \cdot m = 0, \quad m \in \partial B.$$

For theoretical results concerning the existence of solutions of the coupled system we refer to [19, 20]. We are interested in the probability density, which is the practically relevant solution [19].

For some special configuration solutions with small flow rates, the use of moment closure approximations has been investigated by several authors, see e.g. [9, 11, 12, 25]. Most numerical methods developed for the Fokker-Planck equation have been based on the form of (1.3a); see, for example, [1, 2, 10, 24]. Some elaborate numerical algorithms based on spectral methods were recently developed for the Fokker-Planck equation of FENE model in [6, 7, 15]. A spectral Galerkin approximation was further introduced in [14] based on a weighted weak formulation for $f(b - |m|^2)^{-b/4}$. An improved weighted formulation was proposed in [23] in terms of $f(b - |m|^2)^{-s/2}$ for $1 < s \leq b$, leading to a different spectral-Galerkin algorithm. The methods in [14, 23] have provable stability results for certain weighted integrable initial data. However, positivity of the numerical solution is not guaranteed. It is, therefore, desirable to design a method which preserves three important properties of the pdf, that is constant integral (mass conservation), positivity preserving and entropy satisfying. In this paper, we develop such a method.

A key quantity in the design of our numerical method is the relative entropy. To illustrate the idea, we reformulate the Fokker-Planck equation (1.3a). If \mathcal{K} is normal, it can be verified that the equilibrium solution can be determined explicitly as

$$(1.5) \quad M = (b - |m|^2)^{b/2} \exp(m^T \mathcal{K}^s m),$$

where \mathcal{K}^s is the symmetric part of \mathcal{K} . Let \mathcal{K}^a be the asymmetric part of \mathcal{K} , then the Fokker-Planck equation can be rewritten as

$$(1.6) \quad \partial_t f = \frac{1}{2} \nabla_m \cdot (M \nabla_m g - 2\mathcal{K}^a m f), \quad f = gM.$$

Using the zero flux boundary condition (1.4), it can be shown that the relative entropy

$$E(t) := \int_B \frac{f^2}{M} dm = \int_B g^2 M dm,$$

satisfies the following inequality

$$E(t) + \int_0^t \int_B M |\nabla_m g|^2 dm d\tau \leq E(0), \quad \forall t > 0.$$

This ensures that the relative entropy is decreasing in time, and as time evolves the entropy dissipation will drive the solution towards the equilibrium, i.e.,

$$\lim_{t \rightarrow \infty} f(t, m) = CM(m),$$

for some $C > 0$. We refer to [13] for rigorous analysis of long-time asymptotics of the FENE model, and [3] for entropy methods to study rate of convergence to equilibrium for Fokker-Planck type equations. As the

first step, we shall design a finite volume scheme based on (1.6), and show the stability property in terms of the relative entropy.

This paper is organized as follows: in Section 2, we describe the formulation of our scheme for the one dimensional case. Theoretical analysis for both semi-discrete and full discrete schemes is provided. In Section 3, we generalize the scheme to two space dimensions. Implementation strategies are discussed in Section 4. Numerical results of both one and two dimensions are presented in Section 5. Finally, in Section 6, concluding remarks are given.

2. 1-D FOKKER-PLANCK EQUATION

We begin by looking at the Fokker-Planck problem in one dimensional space with $\mathcal{K} = 0$ and $B = (-\sqrt{b}, \sqrt{b})$,

$$(2.1a) \quad \partial_t f = \frac{1}{2} \partial_m^2 f + \frac{1}{2} \partial_m \left(\frac{bm}{b-m^2} f \right), \quad m \in B, t > 0,$$

$$(2.1b) \quad f(m, 0) = f_0(m), \quad m \in B,$$

$$(2.1c) \quad \partial_m f + \frac{bm}{b-m^2} f|_{m=\pm\sqrt{b}} = 0, \quad t > 0.$$

The associated equilibrium solution reduces to

$$M(m) = (b - m^2)^{\frac{b}{2}}, \quad m \in B,$$

and (2.1a) becomes

$$(2.2) \quad \partial_t f = \frac{1}{2} \partial_m (M \partial_m g), \quad \text{where } g = \frac{f}{M}.$$

2.1. Semi-discrete scheme. Given a positive integer N , we partition the domain $(-\sqrt{b}, \sqrt{b})$ by defining the uniform mesh size $h = \frac{2\sqrt{b}}{N}$, and the cell center at

$$m_j = -\sqrt{b} + (j - \frac{1}{2})h, \quad 1 \leq j \leq N.$$

Notice that at two end points, $M(m_{\frac{1}{2}}) = M(m_{N+\frac{1}{2}}) = 0$, and $M(m_{j+\frac{1}{2}}) > 0$ for $1 \leq j \leq N-1$. On each computational cell $I_j = [m_{j-\frac{1}{2}}, m_{j+\frac{1}{2}}]$, we define the cell average of f as

$$\bar{f}_j(t) = \frac{1}{h} \int_{I_j} f(m, t) dm.$$

Integration of (2.2) on I_j yields

$$\frac{d}{dt} \bar{f}_j = \frac{1}{2h} \int_{I_j} \partial_m (M \partial_m g) dm = \frac{1}{2h} M \partial_m g \Big|_{m_{j-\frac{1}{2}}}^{m_{j+\frac{1}{2}}}.$$

Based on this formulation we derive a finite volume scheme to compute $\{f_j\}$ which approximates $\{\bar{f}_j\}$ by taking the numerical flux

$$(2.3) \quad J_{j+\frac{1}{2}} = \widehat{M \partial_m g} = M_{j+\frac{1}{2}} \frac{1}{h} (g_{j+1} - g_j) \quad \text{for } j = 1, \dots, N-1$$

with $M_{j+\frac{1}{2}} := M(m_{j+\frac{1}{2}})$, $g_j(t) = \frac{f_j(t)}{M_j}$. We also set

$$(2.4) \quad J_{\frac{1}{2}} = J_{N+\frac{1}{2}} = 0$$

to incorporate the zero flux at the boundary.

Then we obtain a semi-discrete scheme

$$(2.5) \quad \begin{aligned} \frac{d}{dt} f_1 &= \frac{1}{2h} J_{\frac{3}{2}}, \\ \frac{d}{dt} f_j &= \frac{1}{2h} (J_{j+\frac{1}{2}} - J_{j-\frac{1}{2}}), \quad 2 \leq j \leq N-1, \\ \frac{d}{dt} f_N &= -\frac{1}{2h} J_{N-\frac{1}{2}}, \end{aligned}$$

subject to the initial data

$$f_j(0) = \frac{1}{h} \int_{I_j} f_0(m) dm, \quad j = 1, \dots, N.$$

Theorem 2.1. *The semi-discrete scheme (2.5) satisfies the following properties:*

- (1) *Conservation of mass:* $\sum_{j=1}^N f_j(t)h = \sum_{j=1}^N f_j(0)h = \int_B f_0(m) dm, \quad \forall t > 0.$
- (2) *Positivity preserving:* *for any $t > 0$, $f_j(t) \geq 0$ if $f_j(0) \geq 0$.*
- (3) *The relative entropy $E(t) = \sum_{j=1}^N \frac{f_j^2}{M_j} h$ is non-increasing in time, with*

$$\frac{d}{dt} E(t) = - \sum_{j=1}^{N-1} \frac{h J_{j+\frac{1}{2}}^2}{M_{j+\frac{1}{2}}} \leq 0.$$

Proof. (1) Summing all equations in (2.5), we have

$$\frac{d}{dt} \sum_{j=1}^N f_j(t) = \sum_{j=1}^N \frac{d}{dt} f_j(t) = 0.$$

So

$$\sum_{j=1}^N f_j(t)h = \sum_{j=1}^N f_j(0)h = \int_B f_0(m) dm.$$

- (2) Since M_j is independent of t , we have $\frac{d}{dt} f_j = M_j \frac{d}{dt} g_j$. The scheme (2.5) can be rewritten as

$$(2.6) \quad \begin{aligned} \frac{d}{dt} g_1 &= \frac{1}{2h^2 M_1} M_{\frac{3}{2}} (g_2 - g_1), \\ \frac{d}{dt} g_j &= \frac{1}{2h^2 M_j} [M_{j+\frac{1}{2}} (g_{j+1} - g_j) - M_{j-\frac{1}{2}} (g_j - g_{j-1})], \quad 2 \leq j \leq N-1, \\ \frac{d}{dt} g_N &= -\frac{1}{2h^2 M_N} M_{N-\frac{1}{2}} (g_N - g_{N-1}). \end{aligned}$$

From (1), we see that

$$\sum_{j=1}^N M_j g_j(t) = \sum_{j=1}^N f_j(0), \quad \forall t > 0.$$

Then all the trajectories of (2.6) remain on this hyperplane. We define a closed set on this hyperplane by

$$\Sigma = \left\{ \vec{g} : g_j \geq 0, j = 1, \dots, N, \text{ and } \sum_{j=1}^N M_j g_j = \sum_{j=1}^N f_j(0) \right\}.$$

Let $\vec{F}(\vec{g})$ be the vector field defined by the right hand side of (2.6), then

$$\frac{d}{dt} \vec{g} = \frac{1}{2} \vec{F}(\vec{g}).$$

It suffices to show that Σ is an invariant region of this system. This is indeed the case, if the vector field $\vec{F}(\vec{g})$ points strictly into Σ on the boundary $\partial\Sigma$, i.e., for any outward normal vector \vec{n} on any part of $\partial\Sigma$,

$$\vec{F}(\vec{g}) \cdot \vec{n} < 0.$$

From (2.6), it follows that

$$(2.7) \quad \begin{aligned} \vec{F}(\vec{g}) \cdot \vec{n} &= \sum_{j=1}^{N-1} \frac{n_j}{h^2 M_j} M_{j+\frac{1}{2}} (g_{j+1} - g_j) - \sum_{j=2}^N \frac{n_j}{h^2 M_j} M_{j-\frac{1}{2}} (g_j - g_{j-1}), \\ &= -\frac{1}{h^2} \sum_{j=1}^{N-1} \left(\frac{n_{j+1}}{M_{j+1}} - \frac{n_j}{M_j} \right) M_{j+\frac{1}{2}} (g_{j+1} - g_j). \end{aligned}$$

For each $\vec{g} \in \Sigma$, we define the set of indices S such that

$$S = \{1 \leq j \leq N : g_j = 0\},$$

which implies that $S \neq \emptyset$ for any $\vec{g}_b \in \partial\Sigma$. Then the outward normal vectors \vec{n} at \vec{g}_b are of the form

$$\vec{n} = (n_1, \dots, n_N)^T \quad \text{with} \quad n_j = \begin{cases} -\alpha_j, & \text{if } j \in S, \\ M_j, & \text{if } j \notin S. \end{cases}$$

Furthermore, there exists a positive real number γ such that $\vec{g}_b - \gamma\vec{n}$ is in the interior of Σ , which implies that

$$\alpha_j > 0, \quad j \in S,$$

and

$$\sum_{j=1}^N M_j n_j = 0, \quad \text{i.e.,} \quad \sum_{j \in S} M_j \alpha_j = \sum_{j \notin S} M_j^2.$$

Now we look back at (2.7). Note that if $j, j+1 \in S$, then $g_j = g_{j+1} = 0$; if $j, j+1 \notin S$, then $\frac{n_{j+1}}{M_{j+1}} - \frac{n_j}{M_j} = 1 - 1 = 0$. Therefore the nonzero terms in (2.7) are only those with $j \in S, j+1 \notin S$ or $j \notin S, j+1 \in S$. Hence

$$\begin{aligned} \vec{F}(\vec{g}) \cdot \vec{n} &= -\frac{1}{h^2} \left(\sum_{\substack{j \in S \\ j+1 \notin S}} + \sum_{\substack{j \notin S \\ j+1 \in S}} \right) \left(\frac{n_{j+1}}{M_{j+1}} - \frac{n_j}{M_j} \right) M_{j+\frac{1}{2}} (g_{j+1} - g_j) \\ &= -\frac{1}{h^2} \sum_{\substack{j \in S \\ j+1 \notin S}} \left(1 + \frac{\alpha_j}{M_j} \right) M_{j+\frac{1}{2}} g_{j+1} - \frac{1}{h^2} \sum_{\substack{j \notin S \\ j+1 \in S}} \left(1 + \frac{\alpha_{j+1}}{M_{j+1}} \right) M_{j+\frac{1}{2}} g_j < 0. \end{aligned}$$

This leads to the conclusion that $g_j(t) \geq 0$ as long as $g_j(0) \in \Sigma$.

(3) We now show that the relative entropy $E(t)$ is non-increasing. In fact,

$$\begin{aligned} \frac{d}{dt} \sum_{j=1}^N \frac{f_j^2}{M_j} h &= 2 \sum_{j=1}^N \frac{f_j}{M_j} \frac{d}{dt} f_j h = \sum_{j=1}^N g_j (J_{j+\frac{1}{2}} - J_{j-\frac{1}{2}}) \\ &= - \sum_{j=1}^{N-1} (g_{j+1} - g_j) J_{j+\frac{1}{2}} \\ &= - \sum_{j=1}^{N-1} \frac{h J_{j+\frac{1}{2}}^2}{M_{j+\frac{1}{2}}} \leq 0. \end{aligned}$$

□

We may also examine the large time behavior of $t \rightarrow \vec{g}(t)$. Both positivity $\vec{g}(t) > 0$ and the constraint

$$\sum_{j=1}^N g_j(t) M_j h = \int_B f_0(m) dm$$

together ensure that $\vec{g}(t)$ will remain bounded for all time. Since (2.6) is an autonomous system, what happens as $t \rightarrow \infty$ is simple to describe: for any bounded solution, $\lim_{t \rightarrow \infty} \vec{g}(t)$ becomes the equilibrium solution for every N with $\vec{F}(\vec{g}_{eq}) = 0$. By verification, the only equilibrium solution to (2.6) is $\vec{g}_{eq} = C(1, \dots, 1)^\top$. This leads to the following result.

Theorem 2.2. *Consider the semi-discrete scheme (2.5) subject to the initial data $f_j(0) > 0$ with $\sum_{j=1}^N f_j(0)h = \int_B f_0(m) dm$, then*

$$[f_1, f_2, \dots, f_N]^\top \rightarrow C[M_1, \dots, M_N], \quad t \rightarrow \infty,$$

where

$$C = \frac{\int_B f_0(m) dm}{\sum_{j=1}^N M_j h}.$$

2.2. Fully discrete scheme. Let the time step be denoted by k , and the mesh ratio $\lambda = \frac{k}{2h^2}$. We apply the backward Euler method to the semi-discrete scheme (2.5) to get

$$(2.8) \quad \begin{aligned} f_1^{n+1} &= f_1^n + \lambda M_{\frac{3}{2}} (g_2^{n+1} - g_1^{n+1}), \\ f_j^{n+1} &= f_j^n + \lambda \left[M_{j+\frac{1}{2}} (g_{j+1}^{n+1} - g_j^{n+1}) - M_{j-\frac{1}{2}} (g_j^{n+1} - g_{j-1}^{n+1}) \right], 2 \leq j \leq N-1, \\ f_N^{n+1} &= f_N^n - \lambda M_{N-\frac{1}{2}} (g_N^{n+1} - g_{N-1}^{n+1}). \end{aligned}$$

Given $\{f_j^n\}, \{f_j^{n+1}\}$ can be obtained from $f_j^{n+1} = M_j g_j^{n+1}$ where $\{g_j^{n+1}\}$ solves the following linear system:

$$(2.9) \quad \begin{aligned} (M_1 + \lambda M_{\frac{3}{2}})g_1^{n+1} - \lambda M_{\frac{3}{2}}g_2^{n+1} &= f_1^n, \\ -\lambda M_{j-\frac{1}{2}}g_{j-1}^{n+1} + [M_j + \lambda(M_{j+\frac{1}{2}} + M_{j-\frac{1}{2}})]g_j^{n+1} - \lambda M_{j+\frac{1}{2}}g_{j+1}^{n+1} &= f_j^n, 2 \leq j \leq N-1, \\ -\lambda M_{N-\frac{1}{2}}g_{N-1}^{n+1} + (M_N + \lambda M_{N-\frac{1}{2}})g_N^{n+1} &= f_N^n. \end{aligned}$$

Theorem 2.3. *The fully discrete scheme (2.8) has a unique solution $\{f_j^n\}$. Moreover, the solution satisfies the following properties:*

- (1) *Conservation of mass:* $\sum_{j=1}^N f_j^{n+1}h = \sum_{j=1}^N f_j^n h.$
- (2) *Positivity.* *If $f_j^n \geq 0$, then $f_j^{n+1} \geq 0$.*
- (3) *The relative entropy*

$$E^n = \sum_{j=1}^N \frac{(f_j^n)^2}{M_j} h$$

is nonincreasing. More precisely,

$$(2.10) \quad E^{n+1} = E^n - kh \sum_{j=1}^{N-1} \frac{(J_{j+\frac{1}{2}}^{n+1})^2}{M_{j+\frac{1}{2}}} - \sum_{j=1}^N \frac{(f_j^{n+1} - f_j^n)^2}{M_j} h.$$

Proof. First of all, we show the existence of a solution to (2.8). (2.9) is a linear system of $A\vec{g}^{n+1} = \vec{f}^n$, where

$$\vec{g}^{n+1} = (g_1^{n+1}, \dots, g_N^{n+1})^T, \quad \vec{f}^n = (f_1^n, \dots, f_N^n)^T.$$

From the fact that A is a strictly diagonally dominant matrix, it follows that there is a unique solution $\vec{g}^{n+1} = A^{-1}\vec{f}^n$ for any \vec{f}^n .

- (1) Summing up the N equations in (2.8) gives

$$\sum_{j=1}^N f_j^{n+1}h = \sum_{j=1}^N f_j^n h.$$

- (2) Since $M_j > 0, 1 \leq j \leq N$, we only need to prove that $g_j^{n+1} \geq 0, \forall j$. It suffices to show that $\min_{1 \leq j \leq N} g_j^{n+1} = g_i^{n+1} \geq 0$. We only show the case $2 \leq i \leq N-1$, as the cases $i=1$ and $i=N$ are similar and simpler,

$$\begin{aligned} f_i^n &= -\lambda M_{i-\frac{1}{2}}g_{i-1}^{n+1} + [M_i + \lambda(M_{i+\frac{1}{2}} + M_{i-\frac{1}{2}})]g_i^{n+1} - \lambda M_{i+\frac{1}{2}}g_{i+1}^{n+1} \\ &\leq -\lambda M_{i-\frac{1}{2}}g_i^{n+1} + [M_i + \lambda(M_{i+\frac{1}{2}} + M_{i-\frac{1}{2}})]g_i^{n+1} - \lambda M_{i+\frac{1}{2}}g_i^{n+1} \\ &= M_i g_i^{n+1}. \end{aligned}$$

Hence, $g_i^{n+1} \geq M_i^{-1} f_i^n \geq 0$.

(3) As for the relative entropy, we calculate

$$\begin{aligned} \sum_{j=1}^N \left[\frac{(f_j^{n+1})^2}{M_j} - \frac{(f_j^n)^2}{M_j} \right] &= \sum_{j=1}^N \frac{(2f_j^{n+1} + f_j^n - f_j^{n+1})(f_j^{n+1} - f_j^n)}{M_j} \\ &= \frac{k}{h} \sum_{j=1}^N g_j^{n+1} (J_{j+\frac{1}{2}}^{n+1} - J_{j-\frac{1}{2}}^{n+1}) - \sum_{j=1}^N \frac{(f_j^{n+1} - f_j^n)^2}{M_j} \\ &= -k \sum_{j=1}^{N-1} \frac{(J_{j+\frac{1}{2}}^{n+1})^2}{M_{j+\frac{1}{2}}} - \sum_{j=1}^N \frac{(f_j^{n+1} - f_j^n)^2}{M_j} \leq 0. \end{aligned}$$

Therefore

$$E^{n+1} = E^n - kh \sum_{j=1}^{N-1} \frac{(J_{j+\frac{1}{2}}^{n+1})^2}{M_{j+\frac{1}{2}}} - \sum_{j=1}^N \frac{(f_j^{n+1} - f_j^n)^2}{M_j} h,$$

which implies that the relative entropy is nonincreasing. \square

Remark 2.1. The entropy dissipation relation (2.10) ensures that the fully discrete scheme (2.8) captures the equilibrium solution. In fact, when relative entropy becomes steady so that $E^n = E^{n+1}$, then

$$J_{j+1/2}^{n+1} = 0, \quad f_j^{n+1} - f_j^n = 0,$$

which together imply that $f_j^n = CM_j$.

3. EXTENSION TO THE MULTI-DIMENSIONAL FENE MODEL

3.1. Reformulation. Let the matrix \mathcal{K} be decomposed into a sum of a symmetric part and an asymmetric part, i.e.,

$$\mathcal{K} = \mathcal{K}^s + \mathcal{K}^a.$$

Define $M(m)$ as

$$(3.1) \quad M(m) = (b - |m|^2)^{\frac{b}{2}} e^{m^T \mathcal{K}^s m},$$

and $g(m, t) = \frac{f(m, t)}{M(m)}$, then the Fokker-Planck equation (1.3a) can be rewritten as

$$(3.2) \quad \partial_t f = \frac{1}{2} \nabla_m \cdot (M \nabla_m g - 2\mathcal{K}^a m f).$$

Lemma 3.1. *Let f be the solution to (3.2). If \mathcal{K} is normal, then $M(m)$ is the equilibrium solution to (3.2). Moreover, the relative entropy $E = \int_B g^2 M dm$ satisfies*

$$(3.3) \quad \frac{d}{dt} E(t) + \int_B M |\nabla_m g|^2 dm = 0.$$

Proof. Using zero flux condition in the evolution of E we find that

$$\begin{aligned} \frac{d}{dt} E &= \int_B 2g \partial_t f dm \\ &= \int_B g \nabla_m \cdot [M \nabla_m g - 2\mathcal{K}^a m f] dm \\ &= - \int_B M |\nabla_m g|^2 dm + 2 \int_B \nabla_m g \cdot \mathcal{K}^a m f dm. \end{aligned}$$

Let B_r be a ball with radius $r < \sqrt{b}$, then using integration by parts we obtain

$$\begin{aligned} 2 \int_{B_r} \nabla_m g \cdot \mathcal{K}^a m f dm &= \int_{B_r} \nabla_m g^2 \cdot \mathcal{K}^a m M dm \\ &= \int_{\partial B_r} g^2 M \mathcal{K}^a m \cdot \frac{m}{|m|} dS - \int_{B_r} g^2 \nabla_m \cdot (\mathcal{K}^a m M) dm \\ &= \int_{B_r} g^2 \mathcal{K}^a m \cdot \nabla_m M dm, \end{aligned}$$

which, in virtue of $\nabla_m M = (2\mathcal{K}^s m - \frac{bm}{b-|m|^2})M$, reduces to

$$\int_{B_r} M g^2 m^\top \mathcal{K}^s \mathcal{K}^a m dm = \frac{1}{4} \int_{B_r} M g^2 m^\top (\mathcal{K}^\top \mathcal{K} - \mathcal{K} \mathcal{K}^\top) m dm.$$

This vanishes if \mathcal{K} is normal. Let $r \rightarrow \sqrt{b}$ we obtain

$$\int_B \nabla_m g \cdot \mathcal{K}^a m f dm = 0,$$

hence the desired estimate (3.3) follows. \square

Remark 3.1. If \mathcal{K} is not normal, the above estimate can still be obtained if we replace M by the equilibrium solution. But in such a case, an explicit expression of the equilibrium solution is not available. With M defined above, we will have

$$0 \neq 2 \int_B \nabla_m g \cdot \mathcal{K}^a m f dm \leq \frac{1}{2} \int_B M |\nabla_m g|^2 dm + 2a^2 b \int_B M g^2 dm.$$

Hence

$$\frac{d}{dt} E + \frac{1}{2} \int_B M |\nabla_m g|^2 dm \leq 2a^2 b E,$$

leading to

$$E(t) \leq e^{2a^2 b t} E(0), \quad \text{for } t > 0.$$

In such a case, E is no longer decreasing, though still bounded in finite time.

In the discretization to follow, we shall focus only on the two-dimensional case, for which \mathcal{K} has the following form,

$$\mathcal{K} = \begin{pmatrix} k_{11} & k_{12} \\ k_{21} & -k_{11} \end{pmatrix},$$

with

$$\mathcal{K}^a = \begin{pmatrix} 0 & \frac{k_{12}-k_{21}}{2} \\ -\frac{k_{12}-k_{21}}{2} & 0 \end{pmatrix} = a \begin{pmatrix} 0 & 1 \\ -1 & 0 \end{pmatrix} \quad \text{with } a = \frac{k_{12}-k_{21}}{2},$$

and

$$\mathcal{K}^s = \begin{pmatrix} k_{11} & \frac{k_{12}+k_{21}}{2} \\ \frac{k_{12}+k_{21}}{2} & -k_{11} \end{pmatrix}.$$

3.2. Discretization in $m \in B$. The domain B can be represented by $[0, \sqrt{b}] \times [0, 2\pi]$ in the polar coordinate system. Partition B into uniform rectangles

$$K_{ij} = \{(r, \theta); r_{i-\frac{1}{2}} \leq r \leq r_{i+\frac{1}{2}}, \theta_{j-\frac{1}{2}} \leq \theta \leq \theta_{j+\frac{1}{2}}\}, \quad 1 \leq i \leq P, 1 \leq j \leq Q,$$

where

$$r_{i+\frac{1}{2}} = i\Delta r, \quad \theta_{j+\frac{1}{2}} = j\Delta\theta,$$

with steps of radius and angle

$$\Delta r = \frac{\sqrt{b}}{P}, \quad \Delta\theta = \frac{2\pi}{Q}.$$

Let the cell average of f on K_{ij} be defined by

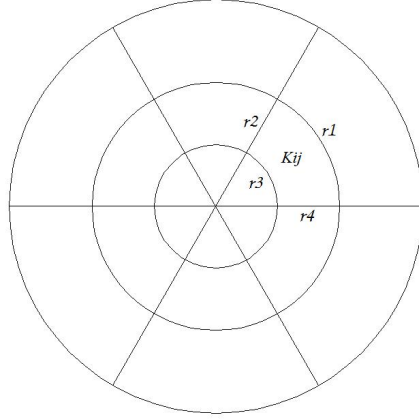
$$\bar{f}_{ij} = \frac{1}{|K_{ij}|} \int_{K_{ij}} f(m, t) dm,$$

where $|K_{ij}| = \Delta\theta\Delta r r_i$ is the area of cell K_{ij} . Integrate (3.2) over K_{ij} on both sides,

$$\begin{aligned} \frac{d}{dt} \bar{f}_{ij} &= \frac{1}{2|K_{ij}|} \int_{K_{ij}} \nabla_m \cdot (M \nabla_m g - 2\mathcal{K}^a m f) dm \\ (3.4) \quad &= \frac{1}{2|K_{ij}|} \int_{\partial K_{ij}} (M \nabla_m g - 2\mathcal{K}^a m f) \cdot \vec{\nu} ds \end{aligned}$$

by the divergence theorem. Here $\vec{\nu}$ is the outward normal of the cell boundary ∂K_{ij} .

In order to derive a finite volume scheme, we use $f_{i,j}$ as the numerical solution in K_{ij} to approximate $\bar{f}_{i,j}$, and represent (3.4) in terms of $\{f_{i,j}\}$.

FIGURE 1. Diagram of the 2D partition of B

Because numerical representatives f and g are not defined on ∂K_{ij} , we need to define a numerical flux to represent $(M\nabla_m g - 2\mathcal{K}^a m f) \cdot \vec{\nu}$ on ∂K_{ij} . To simplify the presentation, we introduce two difference operators,

$$D_r g_{i,j} = \frac{g_{i+1,j} - g_{i,j}}{\Delta r}, \quad D_\theta g_{i,j} = \frac{g_{i,j+1} - g_{i,j}}{\Delta \theta}.$$

There are four pieces within ∂K_{ij} , denoted by $\gamma_1, \gamma_2, \gamma_3$, and γ_4 . On $\gamma_1 = \{(r, \theta); r = r_{i+\frac{1}{2}}, \theta_{j-\frac{1}{2}} \leq \theta \leq \theta_{j+\frac{1}{2}}\}$, we have

$$\begin{aligned} \int_{\gamma_1} M \widehat{\nabla_m g} \cdot \vec{\nu} ds &= \int_{\theta_{j-\frac{1}{2}}}^{\theta_{j+\frac{1}{2}}} M(r_{i+\frac{1}{2}}, \theta) \partial_r g(r_{i+\frac{1}{2}}, \theta) r_{i+\frac{1}{2}} d\theta \\ &= \int_{\theta_{j-\frac{1}{2}}}^{\theta_{j+\frac{1}{2}}} M(r_{i+\frac{1}{2}}, \theta) D_r g_{i,j} r_{i+\frac{1}{2}} d\theta \\ &= \Delta \theta r_{i+\frac{1}{2}} M_{i+\frac{1}{2},j} D_r g_{i,j}, \end{aligned}$$

where we use the midpoint rule for the integration in θ , and $\partial_r g(r_{i+\frac{1}{2}}, \theta) = D_r g_{i,j}$. Similarly, on $\gamma_3 = \{(r, \theta); r = r_{i-\frac{1}{2}}, \theta_{j-\frac{1}{2}} \leq \theta \leq \theta_{j+\frac{1}{2}}\}$,

$$\int_{\gamma_3} M \widehat{\nabla_m g} \cdot \vec{\nu} ds = -\Delta \theta r_{i-\frac{1}{2}} M_{i-\frac{1}{2},j} D_r g_{i-1,j}.$$

On $\gamma_2 = \{(r, \theta); r_{i-\frac{1}{2}} \leq r \leq r_{i+\frac{1}{2}}, \theta = \theta_{j+\frac{1}{2}}\}$, we have $\vec{\nu} = (-\sin \theta, \cos \theta)^T$, and $\nabla_m \cdot \vec{\nu} = \frac{1}{r} \frac{\partial}{\partial \theta}$, hence

$$\begin{aligned} \int_{\gamma_2} M \widehat{\nabla_m g} \cdot \vec{\nu} ds &= \int_{r_{i-\frac{1}{2}}}^{r_{i+\frac{1}{2}}} \frac{M(r, \theta_{j+\frac{1}{2}})}{r} \partial_\theta g(r, \theta_{j+\frac{1}{2}}) dr \\ &= \int_{r_{i-\frac{1}{2}}}^{r_{i+\frac{1}{2}}} \frac{M(r, \theta_{j+\frac{1}{2}})}{r} D_\theta g_{i,j} dr \\ &= \frac{\Delta r M_{i,j+\frac{1}{2}}}{r_i} D_\theta g_{i,j}, \end{aligned}$$

where we have taken $\partial_\theta g(r, \theta_{j+\frac{1}{2}}) = D_\theta g_{i,j}$. Similarly, on $\gamma_4 = \{(r, \theta); r_{i-\frac{1}{2}} \leq r \leq r_{i+\frac{1}{2}}, \theta = \theta_{j-\frac{1}{2}}\}$,

$$\int_{\gamma_4} M \widehat{\nabla_m g} \cdot \vec{\nu} ds = -\frac{\Delta r M_{i,j-\frac{1}{2}}}{r_i} D_\theta g_{i,j-1}.$$

For the asymmetric part,

$$2\mathcal{K}^a m \cdot \vec{\nu} = 2a \begin{pmatrix} 0 & 1 \\ -1 & 0 \end{pmatrix} \begin{pmatrix} m_1 \\ m_2 \end{pmatrix} \cdot \vec{\nu} = \begin{cases} 0, & \text{on } \gamma_1, \\ -2ar, & \text{on } \gamma_2, \\ 0, & \text{on } \gamma_3, \\ 2ar, & \text{on } \gamma_4. \end{cases}$$

It follows that

$$\int_{\partial K_{ij}} (2\mathcal{K}^a m f) \cdot \vec{\nu} ds = -2a \int_{r_{i-\frac{1}{2}}}^{r_{i+\frac{1}{2}}} r f(\widehat{r, \theta_{j+\frac{1}{2}}}) dr + 2a \int_{r_{i-\frac{1}{2}}}^{r_{i+\frac{1}{2}}} r f(\widehat{r, \theta_{j-\frac{1}{2}}}) dr.$$

The numerical flux is chosen to be upwind,

$$f(\widehat{r, \theta_{j+\frac{1}{2}}}) = \frac{1}{2}(f_{i,j+1} + f_{i,j}) + \frac{\text{sgn}(a)}{2}(f_{i,j+1} - f_{i,j}).$$

Hence

$$\int_{\partial K_{ij}} (2\mathcal{K}^a m f) \cdot \vec{\nu} ds = -\Delta r r_i [(a + |a|)(f_{i,j+1} - f_{i,j}) + (a - |a|)(f_{i,j} - f_{i,j-1})].$$

Therefore we obtain the semi-discrete scheme

$$(3.5) \quad \begin{aligned} \frac{d}{dt} f_{i,j} &= \frac{r_{i+\frac{1}{2}} M_{i+\frac{1}{2},j}}{2\Delta r r_i} D_r g_{i,j} - \frac{r_{i-\frac{1}{2}} M_{i-\frac{1}{2},j}}{2\Delta r r_i} D_r g_{i-1,j} + \frac{M_{i,j+\frac{1}{2}}}{2\Delta \theta r_i^2} D_\theta g_{i,j} - \frac{M_{i,j-\frac{1}{2}}}{2\Delta \theta r_i^2} D_\theta g_{i,j-1} \\ &+ \frac{1}{2} [(a + |a|) D_\theta f_{i,j} + (a - |a|) D_\theta f_{i,j-1}]. \end{aligned}$$

In regards to (3.5), when $i = 1$, γ_3 is reduced to a point, so $\frac{r_{\frac{1}{2}} M_{\frac{1}{2},j}}{2\Delta r r_1} D_r g_{0,j}$ is understood as 0; when $i = P$, the zero flux gives that $\frac{r_{P+\frac{1}{2}} M_{P+\frac{1}{2},j}}{2\Delta r r_P} D_r g_{P,j} = 0$. Due to the periodicity of f and M with respect to θ , we take

$$f_{i,j} = f_{i,j+Q}, \quad M_{i,j} = M_{i,j+Q}, \quad \text{for } 1 \leq j \leq Q.$$

Thus (3.5) is well defined for $1 \leq i \leq P, 1 \leq j \leq Q$, which can be solved subject to the initial data

$$f_{i,j}(0) = \frac{1}{|K_{ij}|} \int_{K_{ij}} f_0(m) dm.$$

Theorem 3.2. *Let $\{ij\} = \{1 \leq i \leq P, 1 \leq j \leq Q\}$. The semi-discrete scheme (3.5) has the following two properties:*

- (1) $\sum_{ij} f_{i,j}(t) |K_{ij}| = \sum_{ij} f_{i,j}(0) |K_{ij}| = \int_B f_0(m) dm.$
- (2) *The semi-discrete relative entropy, defined by*

$$E(t) = \sum_{ij} \frac{f_{i,j}^2(t)}{M_{i,j}} |K_{ij}|,$$

satisfies

$$E(t) \leq E(0), \quad t > 0$$

for normal \mathcal{K} ; and $E(t) \leq e^{cat} E(0)$, for general \mathcal{K} with $c > 0$ dependent on b .

Proof. (1) Summation of $\frac{d}{dt} f_{i,j}(t) |K_{ij}|$ over $\{ij\}$ in (3.5) gives

$$\frac{d}{dt} \sum_{ij} f_{i,j}(t) |K_{ij}| = \sum_{ij} \frac{d}{dt} f_{i,j}(t) \Delta \theta \Delta r r_i = 0.$$

So

$$\sum_{ij} f_{i,j}(t) |K_{ij}| = \sum_{ij} f_{i,j}(0) |K_{ij}| = \int_B f_0(m) dm \quad \text{for all } t > 0.$$

(2) Next, we show that $E(t)$ remains bounded for any $t > 0$. For definiteness, we assume $a > 0$.

$$\begin{aligned} \frac{d}{dt}E(t) &= \sum_{ij} 2 \frac{f_{i,j}}{M_{i,j}} \frac{df_{i,j}}{dt} |K_{i,j}| = \sum_{ij} 2g_{i,j} \frac{df_{i,j}}{dt} \Delta\theta \Delta r r_i \\ &= \Delta\theta \sum_{ij} g_{i,j} (r_{i+\frac{1}{2}} M_{i+\frac{1}{2},j} D_r g_{i,j} - r_{i-\frac{1}{2}} M_{i-\frac{1}{2},j} D_r g_{i-1,j}) \\ &\quad + \Delta r \sum_{ij} \frac{g_{i,j}}{r_i} (M_{i,j+\frac{1}{2}} D_\theta g_{i,j} - M_{i,j-\frac{1}{2}} D_\theta g_{i,j-1}) + 2a\Delta r \sum_{ij} g_{i,j} r_i (f_{i,j+1} - f_{i,j}) \\ &= \Delta\theta I + \Delta r II + 2a\Delta r III. \end{aligned}$$

By shifting the indices in i and using $r_{\frac{1}{2}} = 0, M_{P+\frac{1}{2},j} = 0$, we have

$$I = - \sum_{\substack{1 \leq i \leq P-1 \\ 1 \leq j \leq Q}} \Delta r r_{i+\frac{1}{2}} M_{i+\frac{1}{2},j} (D_r g_{i,j})^2 = -\Delta r \sum_{ij} r_{i+\frac{1}{2}} M_{i+\frac{1}{2},j} (D_r g_{i,j})^2.$$

Similarly, shifting the indices in j gives

$$\begin{aligned} II &= - \sum_{\substack{1 \leq i \leq P \\ 1 \leq j \leq Q-1}} \frac{\Delta\theta M_{i,j+\frac{1}{2}}}{r_i} (D_\theta g_{i,j})^2 + \sum_{1 \leq i \leq P} \frac{M_{i,Q+\frac{1}{2}}}{r_i} g_{i,Q} D_\theta g_{i,Q} - \sum_{1 \leq i \leq P} \frac{M_{i,\frac{1}{2}}}{r_i} g_{i,1} D_\theta g_{i,0} \\ &= -\Delta\theta \sum_{ij} \frac{M_{i,j+\frac{1}{2}}}{r_i} (D_\theta g_{i,j})^2. \end{aligned}$$

Here we have used $M_{i,\frac{1}{2}} = M_{i,Q+\frac{1}{2}}, g_{i,1} = g_{i,Q+1}$, and $g_{i,0} = g_{i,Q}$.

Summation by parts in j gives

$$\begin{aligned} III &= - \sum_{ij} (g_{i,j+1} - g_{i,j}) r_i f_{i,j+1} \\ &= - \sum_{ij} r_i M_{i,j+1} g_{i,j+1} (g_{i,j+1} - g_{i,j}) \\ &= -\frac{1}{2} \sum_{ij} r_i M_{i,j+1} (g_{i,j+1} - g_{i,j})^2 + \frac{1}{2} \sum_{ij} r_i g_{ij}^2 (M_{i,j+1} - M_{i,j}). \end{aligned}$$

In 2D case, \mathcal{K} is normal if and only if \mathcal{K} is either symmetric, i.e., $a = 0$, or asymptotic, i.e. $M_{i,j+1} = M_{i,j}$. In either case we have

$$2a\Delta r III \leq 0,$$

hence $\frac{d}{dt}E(t) \leq 0$.

For general matrix \mathcal{K} , we have

$$\frac{d}{dt}E(t) \leq -D(t) + a\Delta r \sum_{ij} r_i g_{ij}^2 (M_{i,j+1} - M_{i,j}),$$

where

$$D(t) = \Delta\theta \Delta r \sum_{ij} r_{i+\frac{1}{2}} M_{i+\frac{1}{2},j} (D_r g_{i,j})^2 + \Delta\theta \Delta r \sum_{ij} \frac{M_{i,j+\frac{1}{2}}}{r_i} (D_\theta g_{i,j})^2.$$

For $A = \max_{\{ij\}} \frac{|M_{i,j+1} - M_{i,j}|}{\Delta\theta M_{i,j}}$,

$$\frac{d}{dt}E(t) \leq -D(t) + \frac{aA}{\beta} E(t).$$

By Gronwall's inequality,

$$E(t) \leq e^{\frac{aA}{\beta}t} E(0) - \int_0^t D(\tau) e^{\frac{aA}{\beta}(t-\tau)} d\tau.$$

□

3.3. Time discretization. We apply the backward Euler method to (3.5), but treating the asymmetric part explicitly,

$$(3.6) \quad \begin{aligned} \frac{f_{i,j}^{n+1} - f_{i,j}^n}{\Delta t} &= \frac{r_{i+\frac{1}{2}} M_{i+\frac{1}{2},j}}{2\Delta r r_i} D_r g_{i,j}^{n+1} - \frac{r_{i-\frac{1}{2}} M_{i-\frac{1}{2},j}}{2\Delta r r_i} D_r g_{i-1,j}^{n+1} + \frac{M_{i,j+\frac{1}{2}}}{2\Delta\theta r_i^2} D_\theta g_{i,j}^{n+1} - \frac{M_{i,j-\frac{1}{2}}}{2\Delta\theta r_i^2} D_\theta g_{i,j-1}^{n+1} \\ &+ \frac{1}{2}[(a + |a|)D_\theta f_{i,j}^n + (a - |a|)D_\theta f_{i,j-1}^n], \end{aligned}$$

with $f_{i,j}^0 = f_{i,j}(0)$. We assume that Δt satisfies the CFL condition

$$(3.7) \quad \frac{|a|\Delta t}{\Delta\theta} \leq 1.$$

Theorem 3.3. *The discrete scheme (3.6) with (3.7) satisfies the following properties:*

- (1) $\sum_{ij} f_{i,j}^n |K_{ij}| = \sum_{ij} f_{i,j}^0 |K_{ij}|, \quad \forall n \in \mathbb{N}.$
- (2) *If the initial data $f_{i,j}^0 \geq 0$, then $f_{i,j}^n \geq 0, \forall n \in \mathbb{N}.$*
- (3) *The discrete relative entropy,*

$$E^n = \sum_{ij} \frac{(f_{i,j}^n)^2}{M_{i,j}} |K_{ij}|,$$

satisfies $E^{n+1} \leq E^n$ for $a = 0$.

Proof. (1) Multiply (3.6) by $|K_{ij}|$, and sum over $\{ij\}$, so that

$$\frac{1}{\Delta t} \left(\sum_{ij} f_{i,j}^{n+1} |K_{ij}| - \sum_{ij} f_{i,j}^n |K_{ij}| \right) = 0.$$

Therefore

$$\sum_{ij} f_{i,j}^{n+1} |K_{ij}| = \sum_{ij} f_{i,j}^n |K_{ij}| = \dots = \sum_{ij} f_{i,j}^0 |K_{ij}|.$$

(2) Rewrite the scheme (3.6) in terms of $g_{i,j}^n$ as follows:

$$(3.8) \quad \begin{aligned} & -\Delta t \frac{r_{i-\frac{1}{2}} M_{i-\frac{1}{2},j}}{2(\Delta r)^2 r_i} g_{i-1,j}^{n+1} - \Delta t \frac{r_{i+\frac{1}{2}} M_{i+\frac{1}{2},j}}{2(\Delta r)^2 r_i} g_{i+1,j}^{n+1} - \Delta t \frac{M_{i,j-\frac{1}{2}}}{2(\Delta\theta)^2 r_i^2} g_{i,j-1}^{n+1} - \Delta t \frac{M_{i,j+\frac{1}{2}}}{2(\Delta\theta)^2 r_i^2} g_{i,j+1}^{n+1} \\ & + (M_{i,j} - (\dots)) g_{i,j}^{n+1} \\ & = -\frac{(a - |a|)\Delta t M_{i,j-1}}{2\Delta\theta} g_{i,j-1}^n + \left(1 - \frac{|a|\Delta t}{\Delta\theta}\right) M_{i,j} g_{i,j}^n + \frac{(a + |a|)\Delta t M_{i,j+1}}{2\Delta\theta} g_{i,j+1}^n, \end{aligned}$$

where (\dots) is the sum of the coefficients of the first four terms on the left-hand side. The CFL condition (3.7) ensures that the right hand side of (3.8) is nonnegative. Note that the coefficient matrix of (3.8) is diagonally dominated. A similar argument to that in 1D case can be applied here to prove that $\{g_{i,j}^{n+1}\}$ are nonnegative. It follows that $\{f_{i,j}^{n+1}\}$ are nonnegative.

(3) For simplicity, we examine only the case when $a = 0$, i.e., \mathcal{K} is symmetric. Then

$$\begin{aligned} E^{n+1} - E^n &= \sum_{ij} \frac{(2f_{i,j}^{n+1} - f_{i,j}^{n+1} + f_{i,j}^n)(f_{i,j}^{n+1} - f_{i,j}^n)}{M_{i,j}} |K_{ij}| \\ &= 2 \sum_{ij} g_{i,j}^{n+1} (f_{i,j}^{n+1} - f_{i,j}^n) |K_{ij}| - \sum_{ij} \frac{(f_{i,j}^{n+1} - f_{i,j}^n)^2}{M_{i,j}} |K_{ij}| \\ &= 2(I + II) - \sum_{ij} \frac{(f_{i,j}^{n+1} - f_{i,j}^n)^2}{M_{i,j}} |K_{ij}|, \end{aligned}$$

where

$$\begin{aligned}
I &= \sum_{ij} g_{i,j}^{n+1} \left(\frac{r_{i+\frac{1}{2}} M_{i+\frac{1}{2},j}}{2\Delta r r_i} D_r g_{i,j}^{n+1} - \frac{r_{i-\frac{1}{2}} M_{i-\frac{1}{2},j}}{2\Delta r r_i} D_r g_{i-1,j}^{n+1} \right) |K_{ij}| \Delta t \\
&= \frac{\Delta\theta\Delta t}{2} \left(\sum_{ij} g_{i,j}^{n+1} r_{i+\frac{1}{2}} M_{i+\frac{1}{2},j} D_r g_{i,j}^{n+1} - \sum_{ij} g_{i+1,j}^{n+1} r_{i+\frac{1}{2}} M_{i+\frac{1}{2},j} D_r g_{i,j}^{n+1} \right) \\
&= -\frac{\Delta\theta\Delta r\Delta t}{2} \sum_{ij} r_{i+\frac{1}{2}} M_{i+\frac{1}{2},j} (D_r g_{i,j}^{n+1})^2 \leq 0,
\end{aligned}$$

and similarly, by shifting the index in j , we have

$$\begin{aligned}
II &= \sum_{ij} g_{i,j}^{n+1} \left(\frac{M_{i,j+\frac{1}{2}}}{2\Delta\theta r_i^2} D_\theta g_{i,j}^{n+1} - \frac{M_{i,j-\frac{1}{2}}}{2\Delta\theta r_i^2} D_\theta g_{i,j-1}^{n+1} \right) |K_{ij}| \Delta t \\
&= -\frac{\Delta\theta\Delta r\Delta t}{2} \sum_{ij} \frac{M_{i,j+\frac{1}{2}}}{r_i} (D_\theta g_{i,j}^{n+1})^2 \leq 0.
\end{aligned}$$

So $E^{n+1} \leq E^n$. □

4. IMPLEMENTATION STRATEGIES

4.1. 1-D scheme. We apply the tridiagonal matrix algorithm (also known as the Thomas algorithm) to scheme (2.9). The computation cost is $O(N)$.

4.2. 2-D scheme.

4.2.1. Direct method. A direct method is to solve the linear system $Ax = b$ with a sparse $N \times N$ coefficient matrix with $N = PQ$. If the final time t is a multiple of the time step Δt , the coefficient matrix is the same for each time step. So we only need to compute the LU decomposition once. Furthermore, for large N , the sparsity of coefficient matrix reduces the complexity significantly, which is about $O(P^3Q)$. Solving the decomposed system $LUx = b$ for the solution costs $O(N^2)$. So the total complexity is $O(N^2)$.

4.2.2. Fourier method for $\mathcal{K} = 0$. When no fluid is involved, i.e., $\mathcal{K} = 0$, M is independent of θ , and we denote $M_{i,j}$ by M_i . Then scheme (3.6) can be simplified as

$$\begin{aligned}
(4.1) \quad M_i g_{i,j}^n &= -\Delta t \frac{r_{i-\frac{1}{2}} M_{i-\frac{1}{2}}}{2(\Delta r)^2 r_i} g_{i-1,j}^{n+1} - \Delta t \frac{r_{i+\frac{1}{2}} M_{i+\frac{1}{2}}}{2(\Delta r)^2 r_i} g_{i+1,j}^{n+1} + (M_i - *) g_{i,j}^{n+1} \\
&\quad - \Delta t \frac{M_i}{2(\Delta\theta)^2 r_i^2} (g_{i,j-1}^{n+1} - 2g_{i,j}^{n+1} + g_{i,j+1}^{n+1}),
\end{aligned}$$

where $*$ is the sum of the coefficients of the first two terms on the right hand side. We can use Fourier method in θ to reduce the computation cost.

Set

$$g_{i,j} = \sum_{l=1}^Q \hat{g}_{i,l} e^{-\mathbf{i}(j-1)(l-1)\Delta\theta}, \quad \mathbf{i} = \sqrt{-1}.$$

Its inverse is

$$\hat{g}_{i,l} = \frac{1}{Q} \sum_{j=1}^Q g_{i,j} e^{\mathbf{i}(j-1)(l-1)\Delta\theta}.$$

Applying this to (4.1), one finds an equation for $\hat{g}_{i,l}$,

$$\begin{aligned}
(4.2) \quad M_i \hat{g}_{i,l}^{n+1} &= -\Delta t \frac{r_{i-\frac{1}{2}} M_{i-\frac{1}{2}}}{2(\Delta r)^2 r_i} \hat{g}_{i-1,l}^{n+1} - \Delta t \frac{r_{i+\frac{1}{2}} M_{i+\frac{1}{2}}}{2(\Delta r)^2 r_i} \hat{g}_{i+1,l}^{n+1} + (M_i - *) \hat{g}_{i,l}^{n+1} \\
&\quad - \Delta t \frac{M_i}{2(\Delta \theta)^2 r_i^2} \hat{g}_{i,l}^{n+1} (e^{\mathfrak{i}(l-1)\Delta\theta} - 2 + e^{-\mathfrak{i}(l-1)\Delta\theta}) \\
&= -\Delta t \frac{r_{i-\frac{1}{2}} M_{i-\frac{1}{2}}}{2(\Delta r)^2 r_i} \hat{g}_{i-1,l}^{n+1} - \Delta t \frac{r_{i+\frac{1}{2}} M_{i+\frac{1}{2}}}{2(\Delta r)^2 r_i} \hat{g}_{i+1,l}^{n+1} \\
&\quad + \left[M_i - * + 2\Delta t \frac{M_i}{(\Delta \theta)^2 r_i^2} \sin^2 \left(\frac{(l-1)\Delta\theta}{2} \right) \right] \hat{g}_{i,l}^{n+1}.
\end{aligned}$$

For each l , we obtain a linear system of $(\hat{g}_{1,l}^{n+1}, \dots, \hat{g}_{P,l}^{n+1})^T$. Notice that the coefficient matrix is diagonally dominant, so there exists a unique solution.

The Fourier transform and the inverse Fourier transform need $O(PQ^2)$ operations. And for each time step, the computational cost of solving Q linear systems is $O(QP)$, since they all have a tri-diagonal coefficient matrix. So the total complexity is $O(PQ^2)$, which with complexity $O(N^{1.5})$ is clearly faster than the direct solver described above.

5. NUMERICAL RESULTS

In this section, we provide numerical results to demonstrate i) accuracy of the schemes, ii) capacity to capture equilibrium solutions and large time behavior of the solution, and iii) effects of some typical homogeneous flows.

Denote the initial function without normalization by $\tilde{f}_0(m)$, and the normalized initial data by $f_0(m) = Z^{-1} \tilde{f}_0(m)$, where Z is a normalization factor defined by

$$Z = \int_B \tilde{f}_0(m) dm.$$

We also denote $Z_M = \int_B M(m) dm$.

5.1. 1-D tests. Denote the numerical solution by f_j^n , and the exact solution by $f(m_j, t_n)$.

Definition 1. L_1 error is given by

$$\sum_{j=1}^N |f_j^n - f(m_j, t_n)| h,$$

and L_∞ error is given by

$$\max_{1 \leq j \leq N} |f_j^n - f(m_j, t_n)|.$$

When the exact solution is not available, we replace $f(m_j, t_n)$ by a reference solution to compute the errors.

5.1.1. Accuracy. We illustrate accuracy of scheme (2.9) with several choices of initial data.

Example 1. In this example, we consider four kinds of initial data.

- (i) $\tilde{f}_0(m) = (b - m^2)^{\alpha b}$, $\alpha = \frac{1}{4}, \frac{1}{2}, \frac{3}{2}$,
- (ii) the distance function $\tilde{f}_0(m) = \sqrt{b} - |m|$,
- (iii) the characteristic function $\tilde{f}_0(m) = \chi_{[-\sqrt{b}+\varepsilon, \sqrt{b}-\varepsilon]}$, $0 < \varepsilon < \sqrt{b}$, and
- (iv) a cosine function $\tilde{f}_0(m) = 1 + \cos\left(\frac{2m\pi}{\sqrt{b}-\varepsilon} + \pi\right)$, $0 < \varepsilon < \sqrt{b}$.

We take the numerical solution with $N = 2560$ as the reference solution. Table 1 shows the results from the above initial data when $b = 16$.

Example 2. We consider the same initial data as in Example 1, but with $b = 50$. The results are given in Table 2.

TABLE 1. Error and order of accuracy for **Example 1** on a uniform mesh of N cells: $b = 16$, $\Delta t = 0.1$, the final time $t = 1.8$.

$\tilde{f}_0(m)$	$(b - m^2)^{\frac{b}{4}}$				$(b - m^2)^{\frac{b}{2}}$			
N	$L_1 Error$	Order	$L_\infty Error$	Order	$L_1 Error$	Order	$L_\infty Error$	Order
20	8.0174E-02		4.8757E-02		8.3743E-02		5.2371E-02	
40	3.9997E-02	1.003	2.4181E-02	1.012	4.1766E-02	1.004	2.6146E-02	1.002
80	1.9987E-02	1.001	1.1898E-02	1.023	2.0870E-02	1.001	1.2877E-02	1.022
160	9.9923E-03	1.000	5.7596E-03	1.047	1.0433E-02	1.000	6.2318E-03	1.047
320	4.9960E-03	1.000	2.6885E-03	1.099	5.2164E-03	1.000	2.9083E-03	1.099
640	2.4980E-03	1.000	1.1522E-03	1.222	2.6082E-03	1.000	1.2464E-03	1.222
$\tilde{f}_0(m)$	$(b - m^2)^{\frac{3b}{2}}$				$\sqrt{b} - m $			
N	$L_1 Error$	Order	$L_\infty Error$	Order	$L_1 Error$	Order	$L_\infty Error$	Order
20	8.6973E-02		5.6422E-02		7.5030E-02		4.3789E-02	
40	4.3360E-02	1.004	2.8024E-02	1.010	3.7437E-02	1.003	2.1752E-02	1.009
80	2.1665E-02	1.001	1.3821E-02	1.020	1.8708E-02	1.001	1.0691E-02	1.025
160	1.0830E-02	1.000	6.6996E-03	1.045	9.3527E-03	1.000	5.1742E-03	1.047
320	5.4150E-03	1.000	3.1279E-03	1.099	4.6762E-03	1.000	2.4143E-03	1.100
640	2.7077E-03	1.000	1.3420E-03	1.221	2.3381E-03	1.000	1.0346E-03	1.223
$\tilde{f}_0(m)$	$\chi_{[-\sqrt{b}+\varepsilon, \sqrt{b}-\varepsilon]}, \varepsilon = 0.1\sqrt{b}$				$1 + \cos\left(\frac{2m\pi}{\sqrt{b}-\varepsilon} + \pi\right), \varepsilon = 0.01\sqrt{b}$			
N	$L_1 Error$	Order	$L_\infty Error$	Order	$L_1 Error$	Order	$L_\infty Error$	Order
20	6.8805E-02		3.9915E-02		6.5382E-02		4.0115E-02	
40	3.4189E-02	1.009	2.0229E-02	0.981	3.2637E-02	1.002	1.9980E-02	1.006
80	1.7045E-02	1.004	9.8706E-03	1.035	1.6308E-02	1.001	9.8975E-03	1.013
160	8.5147E-03	1.001	4.7625E-03	1.051	8.1527E-03	1.000	4.7862E-03	1.048
320	4.2564E-03	1.000	2.2183E-03	1.102	4.0762E-03	1.000	2.2324E-03	1.100
640	2.1281E-03	1.000	9.4669E-04	1.224	2.0381E-03	1.000	9.5645E-04	1.223

TABLE 2. Error and order of accuracy for **Example 2** on a uniform mesh of N cells: $b = 50$, $\Delta t = 0.1$, final time $t = 1.8$.

$\tilde{f}_0(m)$	$(b - m^2)^{\frac{b}{4}}$				$(b - m^2)^{\frac{b}{2}}$			
N	$L_1 Error$	Order	$L_\infty Error$	Order	$L_1 Error$	Order	$L_\infty Error$	Order
20	1.3517E-01		7.5263E-02		1.4470E-01		8.5089E-02	
40	6.7112E-02	1.010	3.7720E-02	0.997	7.1764E-02	1.012	4.3210E-02	0.978
80	3.3499E-02	1.002	1.8666E-02	1.015	3.5811E-02	1.003	2.1337E-02	1.018
160	1.6742E-02	1.001	9.0516E-03	1.044	1.7897E-02	1.000	1.0327E-02	1.047
320	8.3703E-03	1.000	4.2262E-03	1.099	8.9473E-03	1.000	4.8208E-03	1.099
640	4.1850E-03	1.000	1.8109E-03	1.223	4.4735E-03	1.000	2.0662E-03	1.222
$\tilde{f}_0(m)$	$(b - m^2)^{\frac{3b}{2}}$				$\sqrt{b} - m $			
N	$L_1 Error$	Order	$L_\infty Error$	Order	$L_1 Error$	Order	$L_\infty Error$	Order
20	1.5361E-01		9.8096E-02		1.2262E-01		4.9487E-02	
40	7.6052E-02	1.014	4.8310E-02	1.002	5.5069E-02	1.155	2.4455E-02	1.017
80	3.7937E-02	1.003	2.3980E-02	1.011	2.5515E-02	1.110	1.1328E-02	1.110
160	1.8957E-02	1.001	1.1577E-02	1.051	1.2331E-02	1.049	5.3158E-03	1.092
320	9.4774E-03	1.000	5.4093E-03	1.098	6.0948E-03	1.017	2.4473E-03	1.119
640	4.7385E-03	1.000	2.3175E-03	1.223	3.0406E-03	1.003	1.0431E-03	1.230
$\tilde{f}_0(m)$	$\chi_{[-\sqrt{b}+\varepsilon, \sqrt{b}-\varepsilon]}, \varepsilon = 0.01\sqrt{b}$				$1 + \cos\left(\frac{2m\pi}{\sqrt{b}-\varepsilon} + \pi\right), \varepsilon = 0.1\sqrt{b}$			
N	$L_1 Error$	Order	$L_\infty Error$	Order	$L_1 Error$	Order	$L_\infty Error$	Order
20	1.8124E-01		6.8304E-02		1.3265E-01		6.3595E-02	
40	7.7437E-02	1.227	3.0083E-02	1.183	5.4504E-02	1.283	2.9600E-02	1.103
80	3.2340E-02	1.260	1.2198E-02	1.302	2.3665E-02	1.204	1.3434E-03	1.140
160	1.1460E-02	1.497	6.3900E-03	0.933	1.1099E-02	1.092	6.1892E-03	1.118
320	5.0683E-03	1.177	3.0257E-03	1.079	5.4383E-03	1.029	2.8193E-03	1.134
640	2.6200E-03	0.952	1.0941E-03	1.468	2.7023E-03	1.009	1.1926E-03	1.241

5.1.2. *Large time behavior.* The normalized equilibrium solution of the Fokker-Planck equation is

$$f_{eq}(m) = Z_M^{-1} M(m).$$

We define the distance of the solution from the equilibrium as

$$\max_{1 \leq j \leq N} |f_j^n - f_{eq}(m_j)|.$$

Example 3. Take (iv) in Example 1 as the initial data, and let $b = 16$, $\varepsilon = 0.01\sqrt{b}$. The numerical solutions at $t = 0, 1.0, 1.8$ are plotted in Figure 2, which indicate a fast convergence to the equilibrium state. In Table 3 we see that the distance from the equilibrium solution is decreasing. This confirms that the solution converges to the equilibrium solution f_{eq} as time increases.

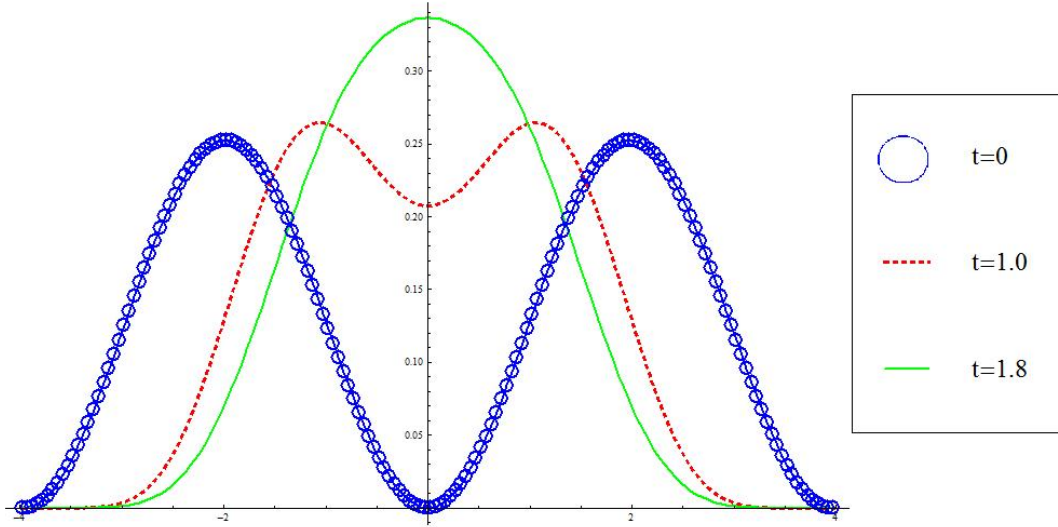


FIGURE 2. $\tilde{f}_0(m) = 1 + \cos\left(\frac{2m\pi}{\sqrt{b}-\varepsilon} + \pi\right)$ with $b = 16, \varepsilon = 0.01\sqrt{b}$

TABLE 3. Numerical convergence to the equilibrium solution measured by distances for **Example 3**: $b = 16, \varepsilon = 0.01\sqrt{b}$, and $N = 160$.

$\tilde{f}_0(m)$ \ t	1	3	4	5	6
$1 + \cos\left(\frac{2m\pi}{\sqrt{b}-\varepsilon} + \pi\right)$	2.0962E-01	1.6390E-02	4.2450E-03	1.0971E-03	2.8348E-04

5.1.3. *Relative entropy.* Now we test the relative entropy of the numerical solutions. The scaled discrete entropy is defined as

$$\sum_{j=1}^N \frac{(f_j^n)^2}{Z_M^{-1} M_j} h.$$

Example 4. We test the time evolution of the relative entropy by using the initial data (i) - (iv) from Example 1. Table 4 shows that the relative entropy is nonincreasing.

TABLE 4. Relative entropy in **Example 4**: $b = 16$, and $N = 640, \Delta t = 0.1$.

$\tilde{f}_0(m)$ \ t	$(b - m^2)^{\frac{b}{4}}$	$(b - m^2)^{\frac{b}{2}}$	$(b - m^2)^{\frac{3b}{2}}$	$\sqrt{b} - m $	$\chi_{[-\sqrt{b}+\varepsilon, \sqrt{b}-\varepsilon]}$ $\varepsilon = 0.1\sqrt{b}$	$1 + \cos\left(\frac{2m\pi}{\sqrt{b}-\varepsilon} + \pi\right)$ $\varepsilon = 0.01\sqrt{b}$
0	1.8141	1	1.3105	1.0129E+12	3346.32	5280.76
0.2	1.2122	1	1.1704	8.3964	35.0358	14.8988
0.6	1.0601	1	1.0575	1.5095	2.9207	3.0020
1.0	1.0207	1	1.0204	1.1435	1.4865	1.6093
1.4	1.0074	1	1.0074	1.0488	1.1608	1.2111
1.8	1.0027	1	1.0027	1.0174	1.0569	1.0755

5.2. **2-D tests.** Denote the numerical solution by $f_{i,j}^n$, and the exact solution by $f(r_i, \theta_j, t_n)$.

Definition 2. L_1 error is given by

$$\sum_{ij} |f_{i,j}^n - f(r_i, \theta_j, t_n)| |K_{ij}|,$$

and L_∞ error is given by

$$\max_{ij} |f_{i,j}^n - f(r_i, \theta_j, t_n)|.$$

Again when the exact solution is not available, we replace $f(r_i, \theta_j, t_n)$ by a reference solution to compute the errors.

The scaled discrete relative entropy is defined by

$$\sum_{ij} \frac{(f_{i,j}^n)^2}{Z_M^{-1} M_{i,j}} |K_{ij}|,$$

and the distance from the equilibrium solution by

$$\max_{ij} |f_{i,j}^n - f_{eq}(r_i, \theta_j)|.$$

5.2.1. *Accuracy test.* If $\mathcal{K} = \mathbf{0}$, we shall apply the method formulated in (4.2).

Example 5. In this test, we consider the two-dimensional problem with $\mathcal{K} = 0, b = 40$, and two types of initial data:

- (i) $\tilde{f}_0(m) = (b - |m|^2)^{\alpha b}$, $\alpha = \frac{1}{4}, \frac{1}{2}, \frac{3}{2}$,
- (ii) $\tilde{f}_0(m) = \cos\left(3\pi \frac{|m|^2}{b}\right) + 1$, and
- (iii) $\tilde{f}_0(m) = M(m)$.

The results are given in Table 5.

TABLE 5. Error and order of accuracy for **Example 5**: $b = 40, \mathcal{K} = 0$, final time $t = 4, \Delta t = 0.05$, the reference solution is given by $P = Q = 320$.

$\tilde{f}_0(m)$	$(b - m^2)^{\frac{b}{4}}$				$(b - m^2)^{\frac{b}{2}}$			
$P = Q$	L_1 Error	Order	L_∞ Error	Order	L_1 Error	Order	L_∞ Error	Order
20	1.0127E-01		1.5472E-02		1.0171E-01		1.5674E-02	
40	5.0798E-02	0.995	7.1504E-03	1.114	5.1013E-02	0.995	7.2466E-03	1.113
80	2.5420E-02	0.999	3.0428E-03	1.223	2.5527E-02	0.999	3.0840E-03	1.232
$\tilde{f}_0(m)$	$(b - m^2)^{\frac{3b}{2}}$				$\cos\left(3\pi \frac{ m ^2}{b}\right) + 1$			
$P = Q$	L_1 Error	Order	L_∞ Error	Order	L_1 Error	Order	L_∞ Error	Order
20	1.0210E-01		1.5845E-02		9.9024E-02		1.4063E-02	
40	5.1202E-02	0.996	7.3289E-03	1.112	4.9565E-02	0.998	6.4869E-03	1.116
80	2.5621E-02	0.999	3.1201E-03	1.232	2.4783E-02	1.000	2.7884E-03	1.218

In Table 6, we choose a symmetric \mathcal{K} with different values of b , and let $\tilde{f}_0(m) = M(m)$. In this particular case, we know that the exact solution is independent of t , which is given by $f_{eq}(m) = Z_M^{-1} M(m)$.

TABLE 6. Error and order of accuracy for **Example 5**: $k_{11} = 0.5, k_{12} = k_{21} = 0.15$, final time $t = 4, \Delta t = 0.05$.

$\tilde{f}_0(m)$	$M(m)$ with $b = 40$				$M(m)$ with $b = 100$			
$P = Q$	L_1 Error	Order	L_∞ Error	Order	L_1 Error	Order	L_∞ Error	Order
10	3.2228E-01		5.1699E-02		4.2884E-01		4.5452E-02	
20	1.6176E-01	0.994	2.6971E-02	0.939	2.1369E-01	1.005	2.6097E-02	0.800
40	8.1719E-02	0.985	1.1744E-02	1.199	1.1278E-01	0.922	1.1779E-02	1.148

5.2.2. *Property test.*

Example 6. Consider the initial data (i) and (ii) in Example 5 with symmetric \mathcal{K} , i.e., $a = 0$. The Fokker-Planck equation has an equilibrium solution $f_{eq}(m) = Z_M^{-1} M(m)$ whose relative entropy is 1. Table 7 shows

TABLE 7. Relative entropy in **Example 6**: $P = Q = 40, b = 40, \mathcal{K} = \mathbf{0}$

t	$\tilde{f}_0(m)$	$(b - m^2)^{\frac{b}{4}}$	$(b - m^2)^{\frac{b}{2}}$	$(b - m^2)^{\frac{3b}{2}}$	$\cos\left(3\pi \frac{ m ^2}{b}\right) + 1$
1		1.06563	1	1.04837	9.25247
2		1.00596	1	1.00448	1.3167
3		1.00056	1	1.00042	1.02827
4		1.00005	1	1.00004	1.00267

that the relative entropy is non-increasing, and converges to 1. Especially, in the second column where we take the equilibrium solution as the initial data, the relative entropy stays the same.

Example 7. Let $a = 0$, i.e. $k_{12} = k_{21}$. Figure 3, obtained from the initial data (ii) in Example 5, illustrates the convergence of the solution towards the equilibrium $f_{eq}(m)$ as t increases. A comparison of solution

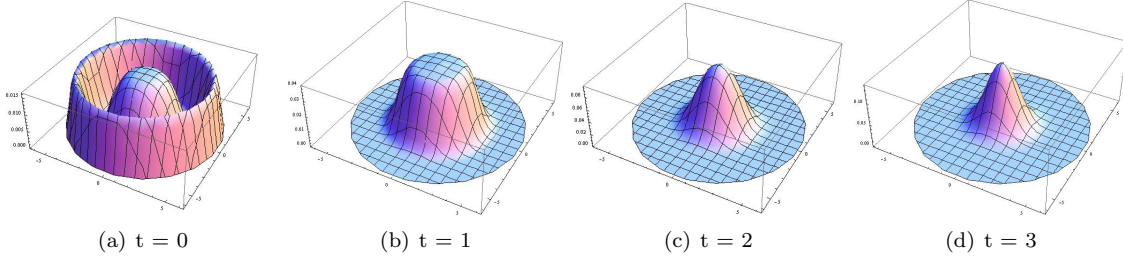


FIGURE 3. $\tilde{f}_0(m) = \cos\left(3\pi\frac{|m|^2}{b}\right) + 1, b = 40, k_{11} = 1.1, k_{12} = 0.15, k_{21} = 0.15, P = Q = 40, \Delta t = 0.05$

TABLE 8. Numerical convergence to the equilibrium solution measured by distances for **Example 7**: $b = 16, k_{11} = 1.1, k_{12} = 0.15, k_{21} = 0.15, \Delta t = 0.05, P = Q = 40$.

$\tilde{f}_0(m) \backslash t$	3	6	9	12	15	18
$(b - m ^2)^{\frac{b}{2}}$	8.80349E-02	1.42082E-02	2.27856E-03	3.75317E-04	7.44458E-05	2.96284E-05
$\cos\left(3\pi\frac{ m ^2}{b}\right) + 1$	4.64376E-02	7.56072E-03	1.30858E-03	3.12548E-04	1.58325E-04	1.37345E-04

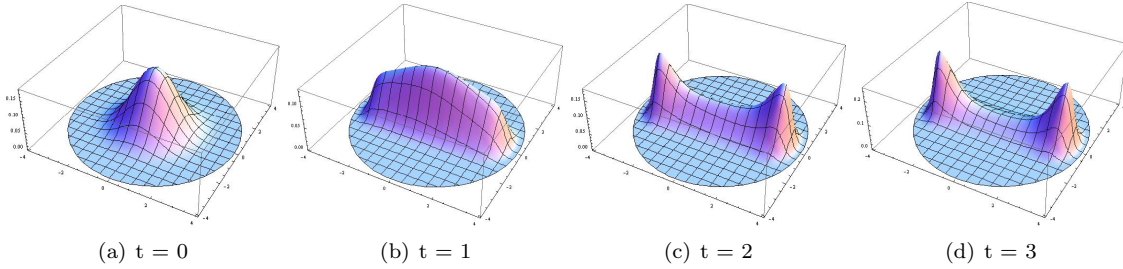


FIGURE 4. $\tilde{f}_0(m) = (b - |m|^2)^{\frac{b}{2}}, b = 16, k_{11} = 1.1, k_{12} = 0.15, k_{21} = 0.15, \Delta t = 0.05$.

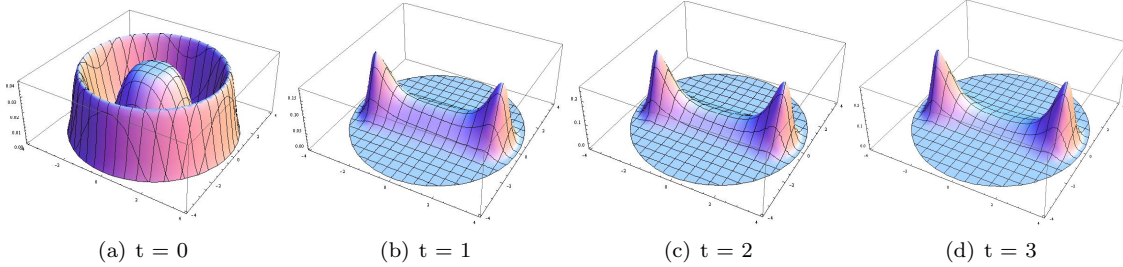


FIGURE 5. $\tilde{f}_0(m) = \cos\left(3\pi\frac{|m|^2}{b}\right) + 1, b = 16, k_{11} = 1.1, k_{12} = 0.15, k_{21} = 0.15, \Delta t = 0.05$.

behavior for two different initial data but with same $b = 16$ is plotted in Figure 4 and Figure 5. Moreover, Table 8 shows that solutions in these two tests converge to the equilibrium solution.

5.2.3. *Flow effects.* Let (x, y) be the macroscopic Eulerian coordinate, and $\nabla = \left(\frac{\partial}{\partial x}, \frac{\partial}{\partial y}\right)^T$, associated with a fluid velocity field $\vec{v}(x, y)$.

Example 8. Simple extensional flow.

We consider a homogeneous planar strain flow with the velocity field

$$\vec{v} = (\alpha x, -\alpha y),$$

where α is the extensional rate. Then the velocity gradient tensor is

$$\mathcal{K} = \nabla \vec{v} = \begin{pmatrix} \alpha & 0 \\ 0 & -\alpha \end{pmatrix}.$$

This flow is irrotational, and forms a strain flow. With this extensional flow, we consider the initial data with four separate peaks, defined by $\tilde{f}_0(m) = \delta_\varepsilon(m)$, where

$$\delta_\varepsilon(m) = \begin{cases} \left[\frac{\cos\left(\frac{\pi(m_1 - m_{10})}{\varepsilon}\right) + 1}{2\varepsilon} \right] \times \left[\frac{\cos\left(\frac{\pi(m_2 - m_{20})}{\varepsilon}\right) + 1}{2\varepsilon} \right], & |m_1 - m_{10}| \leq \varepsilon \text{ and } |m_2 - m_{20}| \leq \varepsilon, \\ 0, & \text{elsewhere,} \end{cases}$$

where $(m_{10}, m_{20}) \in \{(\pm\beta, 0), (0, \pm\beta)\}$ and $\varepsilon < \beta < \sqrt{b} - \varepsilon$.

Note that in such a case the normalized equilibrium solution is

$$f(m) = Z_M^{-1} M(m), \quad M(m) = (b - |m|^2)^{b/2} e^{\alpha(x^2 - y^2)}.$$

The solutions at different times are plotted in Figure 6. In these tests we can see that the proposed method can well capture the equilibrium solutions for extensional flows.

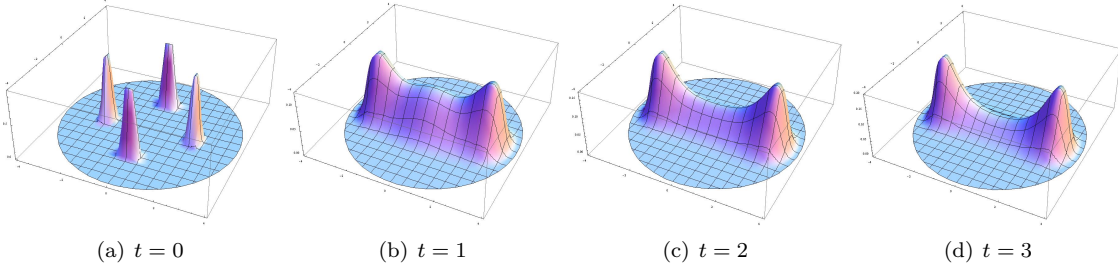


FIGURE 6. $\tilde{f}_0(m) = \delta_\varepsilon(m)$, $b = 16$, $\alpha = 1.1$, $\varepsilon = 2\Delta r$, $\beta = 2$, $P = Q = 40$, $\Delta t = 0.05$.

The contours in Figure 7 show that how the equilibrium solution $f_{eq}(m) = Z_M^{-1} M(m)$ changes with respect to α . Observe that the two peaks of the equilibrium solution move away from each other as α gets

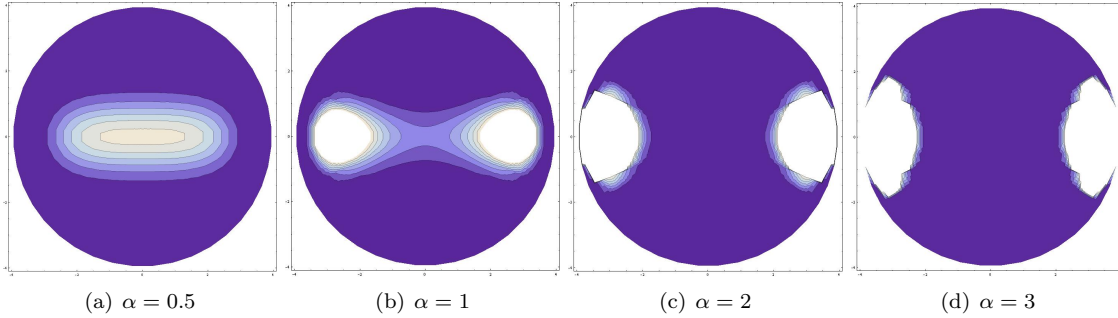


FIGURE 7. $f_{eq}(m) = Z_M^{-1} M(m)$, $b = 16$, $P = Q = 40$

larger.

Example 9. Steady state shear flow.

The steady state shear flow has the velocity field

$$\vec{v} = (\gamma y, 0),$$

where γ is a constant shear rate, and the velocity gradient tensor is

$$\mathcal{K} = \nabla \vec{v} = \begin{pmatrix} 0 & \gamma \\ 0 & 0 \end{pmatrix}.$$

Let $\gamma = 0.1, 0.3, 0.5, 1.0, 2.0$. Figure 8 gives the contour plots of $f_{i,j}^n$ at $t_n = 4$, from which the shear effects are clearly seen. Note that since for shear flow, \mathcal{K} is not normal, we do not expect the scheme to capture

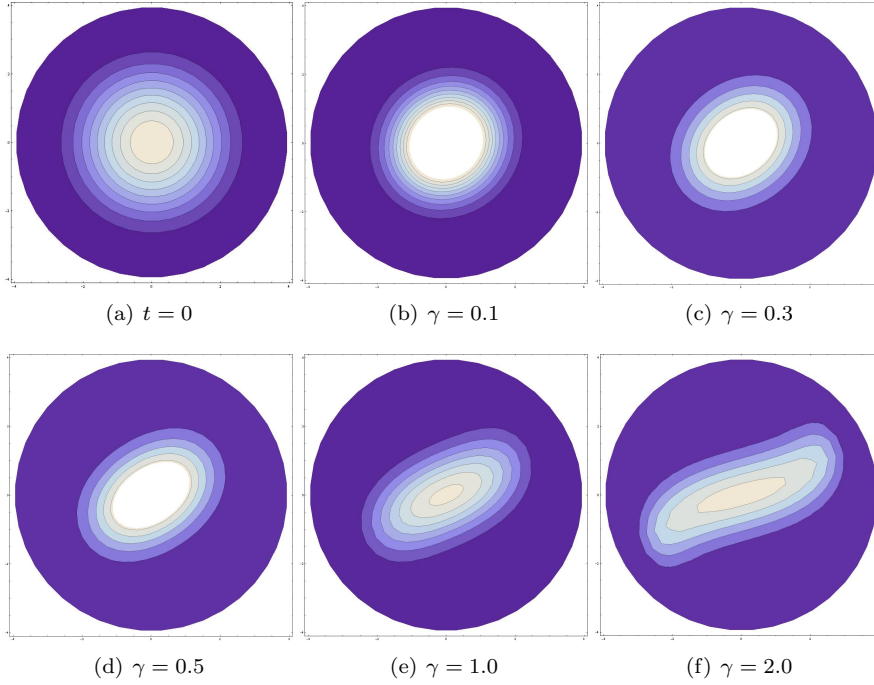


FIGURE 8. The contours of $f_{i,j}^n$ at $t_n = 4$ where $\tilde{f}_0(m) = (b - |m|^2)^{\frac{b}{4}}$, $b = 16$, $P = Q = 40$, $\Delta t = 0.05$.

the large time behavior of the solution.

Example 10. A vortex. A typical vortex has the velocity field

$$\vec{v} = (-\gamma y, \gamma x),$$

with velocity gradient tensor

$$\mathcal{K} = \nabla \vec{v} = \begin{pmatrix} 0 & \gamma \\ -\gamma & 0 \end{pmatrix}.$$

Note that \mathcal{K} is not symmetric, but it is normal, i.e., $\mathcal{K}^T \mathcal{K} = \mathcal{K} \mathcal{K}^T$, hence $f_{eq}(m) = Z_M^{-1} M(m)$ is still an equilibrium solution. In addition, $\mathcal{K}^s = \mathbf{0}$ in this case, so $M(m) = (b - |m|^2)^{\frac{b}{2}}$. Table 9 shows the convergence to f_{eq} as t increases.

TABLE 9. Numerical convergence to the equilibrium solution measured by distances for **Example 10**: $b = 16$, $\gamma = 0.15$, $\Delta t = 0.05$, $P = Q = 40$.

$\tilde{f}_0(m) \backslash t$	1	2	4	6	8
$\delta_\varepsilon(m)$	8.39533E-02	2.44483E-02	2.25787E-03	2.14324E-04	2.03809E-05

6. CONCLUSION

In this paper, we have investigated the Fokker-Planck equation which is of bead-spring type FENE dumbbell model for polymers, with our focus on the development of an entropy satisfying method for the Fokker-Planck equation subject to zero flux on boundary. We constructed simple, easy-to-implement finite volume schemes and proved that they preserve all three desired properties of the pdf, i.e., constant integral (mass conservation), positivity preserving, and entropy satisfying for \mathcal{K} being normal. The goal of our future work is to extend the numerical method and analytical results herein to a higher order discontinuous Galerkin method.

ACKNOWLEDGMENTS

This research was supported by the National Science Foundation under Kinetic FRG grant DMS07-57227.

REFERENCES

- [1] A. Ammar, B. Mokdad, F. Chinesta and R. Keunings. A new family of solvers for some classes of multidimensional partial differential equations encountered in kinetic theory modeling of complex fluids. *J. Non-Newtonian Fluid Mech.*, 139:153–176, 2006.
- [2] A. Ammar, B. Mokdad, F. Chinesta and R. Keunings. A new family of solvers for some classes of multidimensional partial differential equations encountered in kinetic theory modeling of complex fluids. *J. Non-Newtonian Fluid Mech.*, 144:98–121, 2007.
- [3] A. Arnold, P. Markowich, G. Toscani and A. Uniterreiter. On convex Sobolev inequalities and the rate of convergence to equilibrium for Fokker-Planck type equations. *Comm. Partial Differential Equations.*, 26:43–100, 2001.
- [4] R. B. Bird, C. Curtiss, R. C. Armstrong, and O. Hassager. *Dynamics of Polymeric Liquids, Volume 2: Kinetic Theory*. Wiley Interscience, New York, 1987.
- [5] R.B. Bird and J. M Wiest. *Annu. Rev. Fluid Mech.*, 27:169–193, 1995.
- [6] C. Chauvière, and A. Lozinski. Simulation of complex viscoelastic flows using Fokker-Planck equation: 3D FENE model. *J. Non-Newtonian Fluid Mech.* , 122:201–214, 2004.
- [7] C. Chauvière, and A. Lozinski. Simulation of dilute polymer solutions using a Fokker-Planck equation. *J. Comput. Fluids.*, 33:687–696, 2004.
- [8] P. Degond and H. Liu. Kinetic models for polymers with inertial effects. *Netw. Heterog. Media*, 4(4):625–647, 2009.
- [9] Q. Du, C. Liu, and P. Yu. FENE dumbbell model and its several linear and nonlinear closure approximations. *Multiscale Model. Simul.*, 4(3):709–731, 2005.
- [10] X.J. Fan. Viscosity, first normal-stress coefficient, and molecular stretching in dilute polymer solutions. *J. Non-Newtonian FLuid Mech.*, 17(2): 125–144, 1985.
- [11] Y. Hyon, Q. Du, and C. Liu An enhanced macroscopic closure approximation to the micro-macro FENE for polymeric materials. *Multiscale Model. Simul.*, 7:978–1002, 2008.
- [12] M. Herrchen and H.C. Öttinger. A detailed comparison of various FENE dumbbell models. *J. Non-Newtonian FLuid Mech.*, 68(1):17–42, 1997.
- [13] B. Jourdain, T. Lelièvre, C. Le Bris, and F. Otto. Long-time asymptotics of a multiscale model for polymeric fluid flows. *Arch. Ration. Mech. Anal.*, 181:97–148, 2006.
- [14] D. J. Knezevic, and E. Süli. Spectral Galerkin approximation of Fokker-Planck equations with unbounded drift. *ESAIM: M2AN*, 42(3):445–485, 2009.
- [15] A. Lozinski and C. Chauvière. A fast solver for Fokker-Planck equation applied to viscoelastic flows calculations: 2d FENE model. *Journal of Computational Physics*, 189:607–625, 2003.
- [16] M. Laso and H. C Öttinger. Calculation of viscoelastic flow using molecular models: the CONNFFESSIT approach. *J. Non-Newtonian FLuid Mech.*, 47:1–20, 1993.
- [17] C. Liu and H. Liu. Boundary conditions for the microscopic FENE models. *SIAM J. Appl. Math.*, 68(5):1304–1315, 2008.
- [18] H. Liu and J. Shin. Global well-posedness for the microscopic FENE model with a sharp boundary condition arXiv:0905.1142, 2009.
- [19] H. Liu and J. Shin. The Cauchy-Dirichlet problem for the FENE Dumbbell model of polymeric fluids. arXiv:1010.5807, 2010.
- [20] N. Masmoudi. Well-posedness for the FENE dumbbell model of polymeric flows. *Comm. Pure Appl. Math.*, 61(12):1685–1714, 2008.
- [21] H. Öttinger. *Stochastic Processes in Polymeric Liquids*. Springer-Verlag, Berlin and New York, 1996.
- [22] R.G. Owens and T.N. Phillips. *Computational Rheology*. Imperial College Press, London, 2002.
- [23] J. Shen and H. J. Yu. On the approximation of the Fokker-Planck equation of FENE dumbbell model, I: A new weighted formulation and an optimal Spectral-Galerkin algorithm in 2-D. *Preprint*, 2010.
- [24] H. R. Warner. *Ind. Eng. Chem. Fundam.* , 11:379–387, 1972.
- [25] H. Wang, K. Li and P. Zhang. Crucial properties of the moment closure model FENE-QE. *J. Non-Newtonian FLuid Mech.*, 150(2-3):80–92, 2008.

IOWA STATE UNIVERSITY, MATHEMATICS DEPARTMENT, AMES, IA 50011
E-mail address: hliu@iastate.edu

IOWA STATE UNIVERSITY, MATHEMATICS DEPARTMENT, AMES, IA 50011
E-mail address: legendyu@iastate.edu